

Parametric simulations of the metallic double-ring metamaterials: Geometric optimization and terahertz response

Zheng-Gao Dong,^{1,a)} Ming-Xiang Xu,¹ Hui Liu,² Tao Li,² and Shi-Ning Zhu²

¹Physics Department, Southeast University, Nanjing 211189, China

²National Laboratory of Solid State Microstructures, Nanjing University, Nanjing 210093, China

(Received 30 June 2008; accepted 28 December 2008; published online 10 February 2009)

Metallic double-ring metamaterial without splits in both of the rings was recently studied to show its negative refraction with magnetic resonance [Z.-G. Dong *et al.*, Appl. Phys. Lett. **92**, 064101 (2008)]. As a consequent work, systematic numerical results are presented in this paper to investigate the dependence of the magnetically resonant transmission on the structural parameters. The origin of the transmission band with magnetic resonance is shown rather explicitly with these numerical results. In addition, the optimized structure of the double-ring metamaterial is used to explore its terahertz response with all the sizes scaled down simultaneously. © 2009 American Institute of Physics. [DOI: 10.1063/1.3077265]

I. INTRODUCTION

Resonant magnetism from metallic metamaterials is promising for artificial magnetic response at frequencies far above the gigahertz regime,^{1–5} which is of great interest because the magnetic existence in natural materials vanishes gradually with the frequency spectrum going upward.^{6–8} Thanks to the magnetic response in artificial materials, significant progresses have been highlighted in the past decade such as the negative refraction,⁹ superlens,¹⁰ and cloaking effect.¹¹ Magnetic structures composed of various metallic shapes, for example, the double split-ring resonators (DSRRs),^{1,8} split-ring chains,¹² and cut-wire pairs,^{13,14} have been proposed to produce magnetic response. On the one hand, these structures generally have the same mechanism in forming the magnetic response. On the other hand, many variations in these previously proposed structures have been studied intensively in order to design geometrically optimized metallic metamaterials with better electromagnetic performance. For instance, the single-split DSRR was developed to be a single ring resonator with multiple splits and a U-shaped one.¹⁵ Kafesaki *et al.*¹⁶ investigated the fishnet structure and its modified versions. More recently, parametric study shows that the left-handed peak depends strongly on the geometric parameters of the periodic inclusions.¹⁷

In our recent work, a double-ring metamaterial without split in both of the outer and inner rings was confirmed to reveal negative refraction in the magnetically resonant transmission band.¹⁸ The configuration of the double-ring metamaterial with respect to the DSRRs is of interest not only for its convenience in fabrication but also for its isotropic electromagnetic response in the ring plane. It is the objective of this paper, as a consequent work, to explore the optimized response of the double-ring metamaterial. We present systematic numerical results on the magnetic resonance transmission of the double-ring metamaterial to study its geometric dependence. Furthermore, based on the strategy

of geometric optimization, the terahertz response is investigated by scaling down the whole sizes of the double-ring unit proportionally.

II. SIMULATION DETAILS

Figure 1(a) shows schematically the unit cell of the double-ring metamaterial (the square shape of the rings does not introduce qualitative difference with respect to a circular shape). For the purpose of parametric optimization, all the geometric scales are represented by variables, i.e., length of edge a , thickness t , gap g , and widths of the outer-ring edge w_o and inner-ring edge w_i . Additionally, the unit cell has a dimension of $L_x \times L_y \times L_z$, where $L_x = L_y = L$ in consideration of in-plane isotropy of the rings. For consistency and comparability between the gigahertz and terahertz simulations, the metallic rings in the background of vacuum are silver with Drude-type dispersion ($\omega_p = 1.37 \times 10^{16} \text{ s}^{-1}$, $\gamma = 8.5 \times 10^{13} \text{ s}^{-1}$) for all the studies throughout this work. This should not lead to different results in comparison with the perfect conductor approximation in the gigahertz frequencies. In our numerical simulations based on the full-wave finite element method, the simulation configuration has a dimension of $1 \times 1 \times 8$ units (i.e., one unit in the transverse

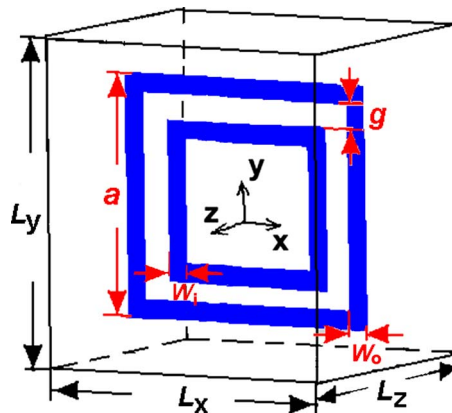


FIG. 1. (Color online) Unit cell of the double-ring metamaterial.

^{a)}Electronic mail: zgdong@seu.edu.cn, <http://dsl.nju.edu.cn/dslweb/images/plasmonics-MPP.htm>.

yz-plane and eight units in the electromagnetic propagation direction along the x -axis). The polarized incident waves with electric field in the y direction and magnetic field in the z direction are satisfied by applying the perfect electric and magnetic boundary conditions, respectively.^{19,20}

III. RESULTS AND DISCUSSIONS

A. Parametric optimization

Optimization of the double-ring metamaterial is needed in order to get a better response of the magnetically resonant transmission such as its bandwidth, magnitude, and quality factor Q . We study the dependence of the magnetically resonant frequency on the structural parameters (i.e., the variables a , w_o , w_i , t , g , L_x , L_y , and L_z) which should be useful to understand the influence of geometry factors on the magnetic resonance and thus obtain an optimization of the magnetic resonance of double rings. According to the different influences on the transmission spectra, two sets of structural parameters can be divided: one set is the scales of the double rings (a , w , t , and g), which contributes mainly to the frequency of the magnetic resonance, while the other set, the unit cell sizes (L_x , L_y , and L_z), determines the frequency regime of the electric stop band, characterized by the electric resonance frequency ω_{eo} and the electric plasma frequency ω_{ep} .^{21,22} Note that the length of the ring edges a contributes not only to the magnetic resonance frequency but also to the frequencies of ω_{eo} and ω_{ep} . In the parametric simulations, the initial values of various variables are as follows: $a = 3.0$ mm, $w_i = w_o = 0.2$ mm, $t = 0.02$ mm, $g = 0.2$ mm, $L_x = L_y = 4.0$ mm, and $L_z = 2.5$ mm.

To interpret the dependence of the magnetic resonance frequency on the geometric configuration, the equivalent LC circuit model can be used to calculate the magnetic resonance frequency $f_0 = 1/(2\pi\sqrt{L_{\text{eff}}C_{\text{eff}}})$. As for the antisymmetric current mode induced in the double rings presented in Ref. 18, L is proportional to the current circulating area [$\approx(2a - 4w_o - 2g)g$] and reversely proportional to the metallic thickness t , while C is proportional to the charge accumulation area [$\approx(a - 2w_o - 2g)t$] and reversely proportional to gap g in analogy to a parallel-plate capacitor. Note that the total effective inductance L_{eff} equals $L/2$ because the left and right inductors are in parallel, while the total effective capacitance C_{eff} equals $C/2$ because the upper and bottom capacitors are in series. Therefore, the inductance, capacitance, and magnetic resonance frequency can be estimated to be

$$L \approx \mu_0\mu(2a - 4w_o - 2g)g/t \quad (1)$$

and

$$C \approx \varepsilon_0\varepsilon(a - 2w_o - 2g)t/g. \quad (2)$$

Consequently,

$$f_0 = \frac{1}{2\pi\sqrt{L_{\text{eff}}C_{\text{eff}}}} = \frac{1}{\pi\sqrt{LC}} \approx \frac{1}{\pi\sqrt{\varepsilon_0\varepsilon\mu_0\mu\sqrt{(2a - 4w_o - 2g)(a - 2w_o - 2g)}}}. \quad (3)$$

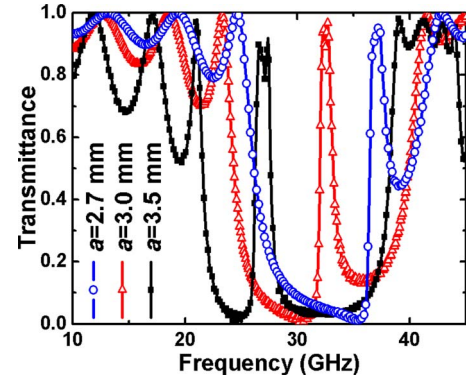


FIG. 2. (Color online) Transmission spectra of the double-ring metamaterial with different lengths of edge a .

Figure 2 shows the transmission spectrum which has been confirmed in our previous work¹⁸ to be a magnetically resonant transmission band occurred within an otherwise stop band from ω_{eo} and ω_{ep} if no magnetic resonance is induced in this regime. Here, we mainly investigate the result of the resonance frequency as a function of the edge length a . As shown in Fig. 2, it is found that the magnetic resonance frequency decreases with the increase in the edge length a , and a further analysis indicates that the resonance frequency is roughly proportional to $1/a$ [see formula (3), consider the approximation of $w_o, g \ll a$].

Figure 3(a) presents the relation between the resonance frequency and the edge width w of the rings. We have assumed that the edge widths of the outer and inner rings have the same value w in Fig. 3(a), and the consequent result reveals that the resonance frequency increases with the width w . However, a further investigation indicates that interestingly, the resonance frequency is rather sensitive to the edge width of the outer ring (w_o) than that of the inner one (w_i). The dependences of the resonance frequency on the width w_o and w_i are shown in Figs. 3(b) and 3(c), respectively. It is clear that modulating the resonance frequency through edge width of the rings can only be realized by w_o . In contrast, it does not show obvious dependence on w_i in consistency with formula (3).

According to the formula (3), larger g will result in higher resonance frequency. This is confirmed in Fig. 4(a), which reveals that the transmission peak moves to higher frequency when the gap g between the inner and outer rings increases. What result accompanies the increased gap is that both the magnitude and the bandwidth of the resonant transmission increase. These increases can be explained by the quality factor $Q = (1/2R)\sqrt{L_{\text{eff}}/C_{\text{eff}}}$ because larger g leads to the increasing of L [see formula (1)] and decreasing of C [see formula (2)], and thus a better Q . This implies that large gap should be preferable to reach sufficient magnitude of the resonant transmission peak. It is worth mentioning that in Fig. 4(a), the changes in gap g is designed by altering the edge length of the inner ring without altering the outer ring. As a matter of fact, an alternative way to change gap g is to alter the edge length of the outer ring while keeping the scale of the inner ring unchanged [Fig. 4(b)]. The discrepant dependence of resonance frequency on gap g between these

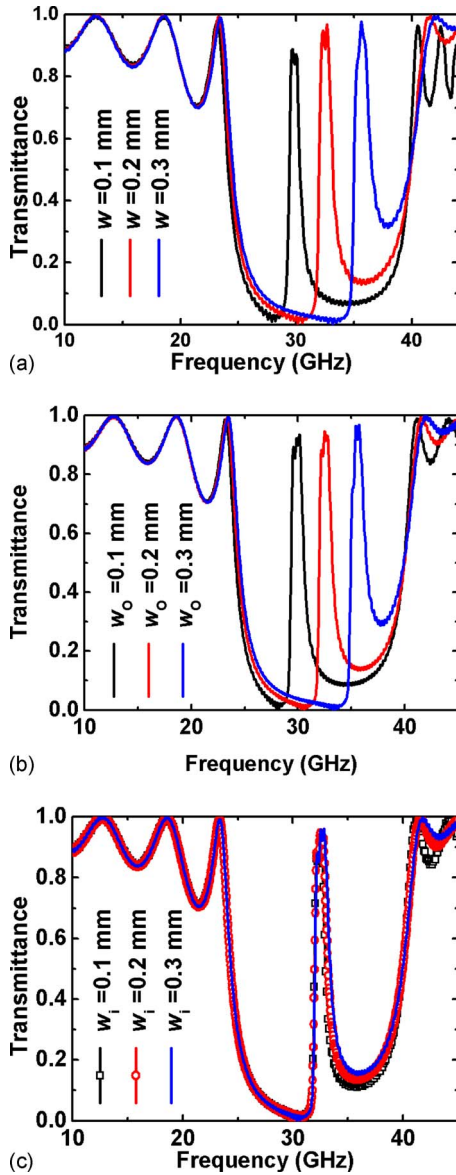


FIG. 3. (Color online) Magnetic resonance frequency as a function of the width of edge w . (a) Dependence on the width w of both outer and inner edges. (b) Dependence on the edge width of outer ring w_o . (c) Dependence on the width of inner edge w_i .

two schemes is caused because the latter has an additional modification of the edge length a , which is inversely proportional to the resonance frequency (see Fig. 2).

Another geometric parameter of the ring shape is its thickness t . In our simulations, the thickness in a large range does not obviously change the magnetically resonance frequency [see formula (3)], except a slight influence on the magnitude of the resonant transmission (Fig. 5). It implies that thinner metallic layer is better to obtain sufficient resonant transmission [i.e., a better quality factor Q , see formulas (1) and (2)]. This result is important for terahertz response since the silver is only an approximately perfect conductor in the microwaves while it gets predominately lossy when the frequencies move to terahertz and above the regime.

As mentioned earlier, in contrast to the magnetically resonant parameters a , w_o , and g of the rings, there is another set of parameters, mainly the periodicity of unit cell, which

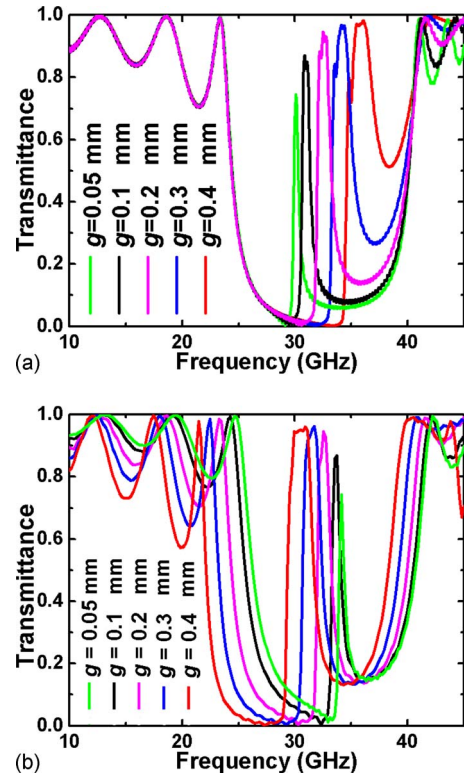


FIG. 4. (Color online) The relation between the resonance frequency and the gap g . (a) Tuning g through the inner ring. (b) Tuning g through the outer ring.

contributes to the stop band caused by electric response. In our previous work,¹⁸ the characteristic of the electric stop band can be described in the way of a cut-wire system. That is, the periodicity of wires determines the magnetic plasma frequency ω_{ep} , while the cut controls the electric resonance frequency ω_{eo} . For the case of electric polarization in the y direction, the cut is controlled by L_y and a (Note that the parameter a has a dual effect on the transmission characteristic). This electric response is confirmed by the simulation result in Fig. 6, from which some conclusions can be summarized. (i) The sizes of unit cell (L_x , L_y , and L_z) do not influence the magnetic resonance frequency. In other words, the magnetic resonance is only related to the shape of the double rings. (ii) The electric stop band is not sensitive to L_z . This is because the metal concentration in the z direction

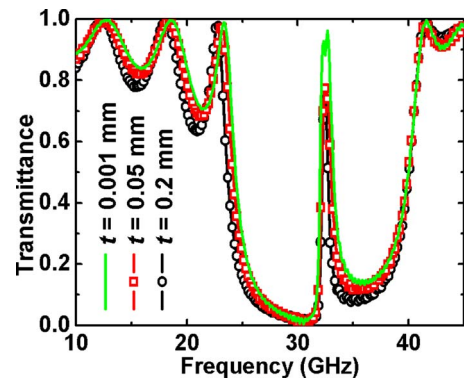


FIG. 5. (Color online) Magnetic resonance frequency as a function of the metallic thickness t .

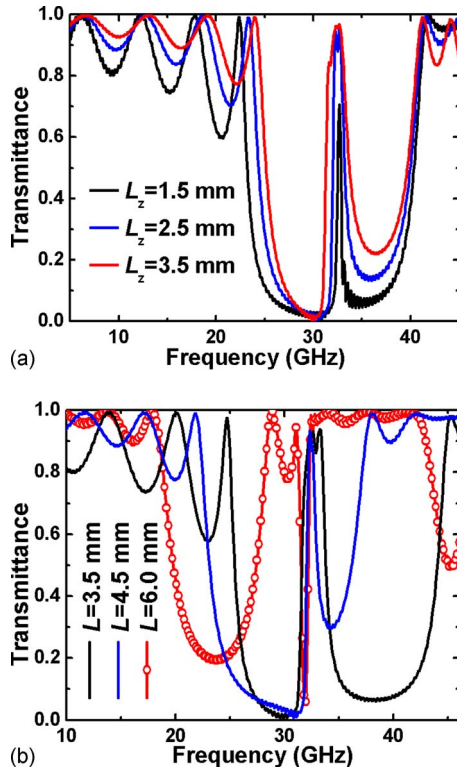


FIG. 6. (Color online) Transmission spectra for various unit cells. (a) Dependence on $L_z (=L_x=L_y)$. (b) Dependence on $L_x=L_y$.

keeps very low while tuning L_z in certain range (for $t \ll L_z$). Nevertheless, it is found that larger L_z results in higher magnitude and wider bandwidth of the resonant transmission peak [see Fig. 6(a)]. (iii) The electric stop band is mainly determined by L_x and L_y . A resonant dip, instead of the resonant peak, will be observed when the electric stop band shifts so far by tuning $L (=L_x=L_y)$, as shown in Fig. 6(b), that the unaltered frequency of magnetic resonance is out of the range from ω_{eo} to ω_{ep} .

B. Terahertz response

In addition to the potential applications in the microwave regime, metamaterials at terahertz frequencies, even infrared and/or visible frequencies are rather attractive and challenging. As the representative works, the optical properties of negative index metamaterials at optical frequencies were studied intensively, for example, in Refs. 23–26. In this work, a general approach to obtain the optical counterpart of the microwave double-ring metamaterial is to scale down the corresponding microwave designs.

In order to obtain a stronger magnitude of the resonant transmission at terahertz frequency, the structural parameters are chosen with a better quality factor Q according to the earlier simulations of geometric optimization: $a=3.0$ mm, $w_i=w_o=0.15$ mm, $g=0.4$ mm, $t=0.02$ mm, and $L_x=L_y=L_z=3.5$ mm. An additional coefficient, the scaling factor s , is used to describe the ratio that shrinks down all the sizes simultaneously. For simplicity, no host material has been considered for the simulations of geometric optimization in microwave regime. However, in consideration that the host material may result in an obvious loss effect when the re-

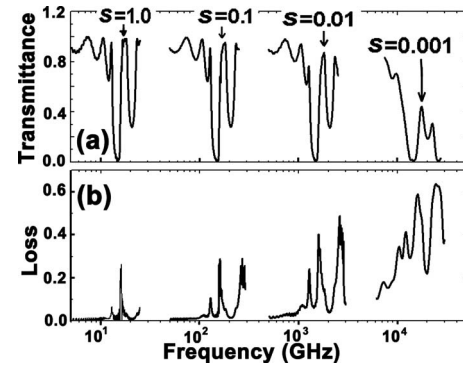


FIG. 7. Terahertz response of the double-ring metamaterial by scaling down all the sizes simultaneously. (a) Transmission spectra. (b) Optical losses.

sponse frequency is at terahertz regime, the metallic rings for scaling purpose are placed in a host material of quartz with permittivity of 3.78 and dielectric loss tangent of 0.0001.

It is found from Fig. 7(a) that when the scaling factor s equals to 1, the resonant transmission peak is located around 17.6 GHz (with a frequency shift factor $\sqrt{\epsilon_{\text{QUARTZ}}}=\sqrt{3.78}$ as compared with the no-host circumstance). As is expected, with the scaling factor s getting smaller, the resonance frequency becomes larger and the peak magnitude of the resonant transmission becomes weaker. Although the result in Fig. 7(a) implies a linear relation between the resonance frequency and the scaling factor s , it should be reminded that the linearity would be broken down for frequencies above 100 THz due to the free electron kinetic energy.^{27,28} It is also clear from Fig. 7(b) that the magnitudes of optical loss become more and more serious when the resonance frequencies move toward the terahertz regime. The resonance loss peaks are much sharper and happen in slightly lower frequencies than the magnetic resonance transmission bands. Higher resonance frequencies are not considered not only because the peak of the resonant transmission will dissipate for the increasing optical losses, but also because the parameters w and t have been scaled down to the state-of-the-art constraint of nanofabrication technologies.

IV. CONCLUSIONS

In conclusion, systematically parametric simulations are performed to investigate the geometric dependence of the resonant transmission as well as the terahertz response by scaling the sizes simultaneously. First, the geometric parameters contribute two aspects to the resonant response. That is, the electric stop band is mainly controlled by the periodicity of the unit cell while the magnetic resonant peak depends only on the sizes of double rings. Second, using the parameters of geometric optimization, linear dependence of the terahertz response on the scaling factor is found up to 18.0 THz.

ACKNOWLEDGMENTS

This work was supported by the National Natural Science Foundation of China (Nos. 10534020, 10604029, 10704036, 10747116, and 10874081). M.-X. Xu also acknowledges the support from the National Science Founda-

tion of Jiangsu Province of China (Grant No. BK2007118).

- ¹T. J. Yen, W. J. Padilla, N. Fang, D. C. Vier, D. R. Smith, J. B. Pendry, D. N. Basov, and X. Zhang, *Science* **303**, 1494 (2004).
- ²S. Linden, C. Enkrich, M. Wegener, J. F. Zhou, T. Koschny, and C. M. Soukoulis, *Science* **306**, 1351 (2004).
- ³S. Zhang, W. Fan, N. C. Panoiu, K. J. Malloy, R. M. Osgood, and S. R. J. Brueck, *Phys. Rev. Lett.* **95**, 137404 (2005).
- ⁴C. Enkrich, M. Wegener, S. Linden, S. Burger, L. Zschiedrich, F. Schmidt, J. F. Zhou, T. Koschny, and C. M. Soukoulis, *Phys. Rev. Lett.* **95**, 203901 (2005).
- ⁵H.-K. Yuan, U. K. Chettiar, W. Cai, A. V. Kildishev, A. Boltasseva, V. P. Drachev, and V. M. Shalaev, *Opt. Express* **15**, 1076 (2007).
- ⁶V. M. Shalaev, *Nat. Photonics* **1**, 41 (2007).
- ⁷F. Magnus, B. Wood, J. Moore, K. Morrison, G. Perkins, J. Fyson, M. C. K. Wiltshire, D. Caplin, L. F. Cohen, and J. B. Pendry, *Nature Mater.* **7**, 295 (2008).
- ⁸J. B. Pendry, A. J. Holden, D. J. Robbins, and W. J. Stewart, *IEEE Trans. Microwave Theory Tech.* **47**, 2075 (1999).
- ⁹D. R. Smith, J. B. Pendry, and M. C. K. Wiltshire, *Science* **305**, 788 (2004).
- ¹⁰X. Zhang and Z. Liu, *Nature Mater.* **7**, 435 (2008).
- ¹¹J. B. Pendry, D. Schurig, and D. R. Smith, *Science* **312**, 1780 (2006).
- ¹²H. Liu, D. A. Genov, D. M. Wu, Y. M. Liu, J. M. Steele, C. Sun, S. N. Zhu, and X. Zhang, *Phys. Rev. Lett.* **97**, 243902 (2006).
- ¹³V. M. Shalaev, W. Cai, U. K. Chettiar, H.-K. Yuan, A. K. Sarychev, V. P. Drachev, and A. V. Kildishev, *Opt. Lett.* **30**, 3356 (2005).
- ¹⁴G. Dolling, C. Enkrich, M. Wegener, J. F. Zhou, and C. M. Soukoulis, *Opt. Lett.* **30**, 3198 (2005); J. F. Zhou, L. Zhang, G. Tuttle, T. Koschny, and C. M. Soukoulis, *Phys. Rev. B* **73**, 041101(R) (2006).
- ¹⁵J. Zhou, T. Koschny, and C. M. Soukoulis, *Opt. Express* **15**, 17881 (2007).
- ¹⁶M. Kafesaki, I. Tsiapa, N. Katsarakis, Th. Koschny, C. M. Soukoulis, and E. N. Economou, *Phys. Rev. B* **75**, 235114 (2007).
- ¹⁷V. D. Lam, J. B. Kim, S. J. Lee, and Y. P. Lee, *J. Appl. Phys.* **103**, 033107 (2008).
- ¹⁸Z.-G. Dong, M. X. Xu, S. Y. Lei, H. Liu, T. Li, F. M. Wang, and S. N. Zhu, *Appl. Phys. Lett.* **92**, 064101 (2008).
- ¹⁹F. M. Wang, H. Liu, T. Li, Z. G. Dong, S. N. Zhu, and X. Zhang, *Phys. Rev. E* **75**, 016604 (2007).
- ²⁰Z. G. Dong, S. N. Zhu, H. Liu, J. Zhu, and W. Cao, *Phys. Rev. E* **72**, 016607 (2005).
- ²¹T. Koschny, M. Kafesaki, E. N. Economou, and C. M. Soukoulis, *Phys. Rev. Lett.* **93**, 107402 (2004).
- ²²J. B. Pendry, A. J. Holden, W. J. Stewart, and I. Youngs, *Phys. Rev. Lett.* **76**, 4773 (1996).
- ²³V. A. Podolskiy, A. K. Sarychev, and V. M. Shalaev, *J. Nonlinear Opt. Phys. Mater.* **11**, 65 (2002).
- ²⁴N. C. Panoiu and R. M. Osgood, *Opt. Commun.* **223**, 331 (2003).
- ²⁵S. O'Brien, D. McPeake, S. A. Ramakrishna, and J. B. Pendry, *Phys. Rev. B* **69**, 241101 (2004).
- ²⁶N. C. Panoiu and R. M. Osgood, *Phys. Rev. E* **68**, 016611 (2003).
- ²⁷J. Zhou, Th. Koschny, M. Kafesaki, E. N. Economou, J. B. Pendry, and C. M. Soukoulis, *Phys. Rev. Lett.* **95**, 223902 (2005).
- ²⁸W. M. Klein, C. Enkrich, M. Wegener, C. M. Soukoulis, and S. Linden, *Opt. Lett.* **31**, 1259 (2006).